Remote supervision and fault detection on OPC monitored PV systems

DOI: 10.1016/j.solener.2016.08.030

Santiago Silvestre[a, *]
Santiago.silvestre@upc.edu

Llanos Mora-López[b]
llanos@lcc.uma.es

Sofiane Kichou[a]
kichousofiane@gmail.com

Francisco Sánchez-Pacheco[c]
fsanchezp@uma.es

Manuel Dominguez-Pumar[a]
Manuel.Dominguez@upc.edu

[a]MNT Group, Electronic Engineering Department, UPC-BarcelonaTech, Barcelona, C/ Jordi Girona 1-3, Mòdul C4 Campus Nord UPC, 08034 Barcelona, Spain

[b]Dpto. Lenguajes y Ciencias de la Computación, Universidad de Málaga, Campus de Teatinos, sn, Málaga 29071, Spain

[c]Dpto. Tecnología Eléctrica, Universidad de Málaga, Campus de Teatinos, sn, Málaga 29071, Spain

*Corresponding author.

Abstract

This paper presents a new approach for automatic supervision and remote fault detection of grid connected photovoltaic (PV) systems by means of OPC technology-based monitoring. The use of standard OPC for monitoring enables data acquisition from a set of devices that use different communication protocols as inverters or other electronic devices present in PV systems enabling universal connectivity and interoperability. Using the OPC standard allows promoting interoperation of software objects in distributed-heterogeneous environments and also allows incorporating in the system remote supervision and diagnosis for the evaluation of grid connected PV facilities. The supervision system analyses the monitored data and evaluates the expected behaviour of main parameters of the PV array: Output voltage, current and power. The monitored data and evaluated parameters are used by the fault detection procedure in order to identify possible faults present in the PV system. The methodology presented has been experimentally validated in the supervision of a grid connected PV system located in Spain. Results obtained show that the combination of OPC monitoring along with the supervision and fault detection procedure is a robust tool that can be very useful in the field of remote supervision and diagnosis of grid connected PV systems. The RMSE between real monitored data and results obtained from the modelling of the PV array were below 3.6% for all parameters even in cloudy days.

Keywords: OPC; Monitoring; Fault detection; PV systems

1 Introduction

One of the main difficulties involved in monitoring systems is the inability to add new devices or new ways of evaluating the performance of these systems without significantly changing the topology of the monitoring system. Firstly, the incorporation of new devices, in the absence of standard communication protocols, requires the development of software for acquiring data from these devices and it is also necessary to add the functionality of each of the data that are acquired. Moreover, in photovoltaic (PV) plants connected to the grid each inverter has its own communication protocol and issues its own program online or locally to access data and plant information. These programs do not allow the inclusion of data from other inverters or for other plants even in the case of inverters from the same manufacturer. Also, it is not possible to

incorporate any functionality to them in order to make a diagnosis and evaluation of the operation of facilities, beyond including the system supplied by the manufacturer of the inverter, who usually simply presents the information of the recorded data. Therefore, it is possible to ensure that one of the most important problems when it comes to monitoring and supervising solar energy plants is the communication between devices due to the different types used. It is common to find many devices of different types and manufacturers who use different ways of communication. In order to obtain a generic system, a general mechanism is needed to communicate with any devices, irrespective of their characteristics or of the manufacturer.

To address these limitations, it has been proposed to use the OPC standard for monitoring PV systems (Martinez-Marchena et al., 2010, 2014). OPC was originally based on OLE (Object Linking and Embedding) for Process Control (Alan Gordon, 2001; Liu et al., 2005). However, OPC is now available on other operating systems. It is a standard and consistent communication system for exchanging information and it allows defining the rules of handshaking between different devices using the client-server paradigm; this system has been used in industry to connect supervisory systems and data acquisition and man-machine interfaces with the physical control systems (Holley, 2004). Moreover, it allows the development of components for interconnecting disperse systems providing interoperability efficiently. This technology enables software components developed by experts in one sector to be used by applications in any other sector. The design of OPC interfaces supports distributed architectures.

The Data access OPC and Historical Data Access specifications are compatible with client-server and publisher-subscriber communication models. The use of the Distributed Component Object Model (DCOM) from Microsoft makes possible the access to remote OPC servers. DCOM extends Microsoft's object-oriented Component Object Model (COM) to promote interoperation of software objects in a distributed-heterogeneous environment.

Using this OPC standard, an automatic assessment model for solar energy plants was proposed in Martínez-Marchena et al., (2014). The model for each installation is built using different data sources. Various daily parameters were proposed to evaluate the performance of a photovoltaic system:

- The daily output energy of the photovoltaic plant, that is, the daily energy supplied by the installation, E_{day}.
- The daily yield, Y_{a_day}, defined as the daily output energy per kW_p installed.

The daily evaluation model is treated as an element of the system. The container used for the model behaves as an OPC client with access to all data.

The operation of each plant is evaluated using a statistical analysis of the differences between the measured parameters and the estimated parameters. These differences are checked using the Jarque-Bera test (Jarque et al., 1987) that informs whether these differences follow a normal distribution. This proposal allows an initial daily evaluation of the performance of the PV system. However, for a complete diagnosis of the detected problems generally related to the DC side of the PV system, it is necessary to use additional methods based on a detailed analysis of monitored data.

A list of fault detection methods for grid connected PV systems was reported in the past. Some of these methods are based on power losses analysis (Chouder and Silvestre, 2010; Drews et al., 2007; Firth et al., 2010) or on theoretical concepts of descriptive and inferential statistics (Vergura et al., 2009; Leloux et al., 2014). Bayesian (Coleman and Zalewski, 2011) and neural networks (Wu et al., 2009) were also used in fault detection procedures. However, these techniques require sophisticated software environments and have a high computational cost. In this work a procedure for automatic fault detection in grid connected PV systems is used. This procedure is based on a technique for the evaluation of current and voltage indicators recently reported that was experimentally validated and can work in real time without using sophisticated software tools (Silvestre et al., 2014, 2015; Chine et al., 2014). The integration of this fault detection procedure along with OPC monitoring, results in a powerful tool for automatic supervision and fault detection of grid connected PV systems. The present work shows the results obtained in the remote supervision of a grid connected PV system with a nominal power of 14.08 kW located in Spain by using diagnosis tools in combination with OPC monitoring.

2 Methodology

2.1 Description of the OPC-based monitoring

The following parameters were monitored: Current, voltage and power (DC and AC), cosine (ϕ), frequency, irradiance, partial energy and module temperature. The irradiance received was measured using a calibrated solar cell installed in the plane of the modules. Module temperature was measured using a Pt100 sensor fitted to the back of the module, in the middle of a cell, near its geometric center. Both parameters are recorded by the data acquisition of the inverter.

All data were supplied by the inverters. For data collection it was used OPC Historical Data Access (OPC HDA) specifications which provide access to information already stored in inverters and allow retrieving this information

in a homogeneous and uniform way. A VPN and IP were used to connect with the facilities. The data collection interval was 5 min. Data are directly retrieved from the inverter. When the inverter is disconnected data are not recorded, but data previously stored in the inverter will be transmitted when the inverter is connected.

Several elements are used in the monitoring process: The client software using OPC HDA technology for downloading data from the devices, the device and the OPC HDA server that knows the protocol and the procedure to download data from the device (Martínez-Marchena, 2015).

Data were stored in a PostgreSQL DBMS compatible with the SQL92 standard. Daily evaluation and fault detection algorithms were implemented with OPC.

2.2 PV system modelling

The model of the PV array is mainly based on the Sandia PV array performance model (SAPM) King et al., 2004. This model is an empirical model described by the fundamental Eqs. (1)–(7). The model contains several coefficients and parameters that are unknown and not provided by the PV module's manufacturer, by knowing these model parameters as well as the solar radiation and the PV modules operating temperature, the output power of the PV array can be predicted by using the following equations:

$$Ee = G/G_n \tag{1}$$

$$Iscg = N_{pg}\left[Isco\cdot Ee\cdot\{1+\alpha_{Isc}\cdot(Tc-To)\}\right] \tag{2}$$

$$Impg = N_{pg}\left[Impo\cdot\left\{C_0\cdot Ee + C_1\cdot Ee^2\right\}\cdot\left\{1+\alpha_{Imp}\cdot(Tc-To)\right\}\right] \tag{3}$$

$$\delta(Tc) = n\cdot k\cdot(Tc+273.15)/q \tag{4}$$

$$Vocg = N_{sg}\left[Voco + N_s\cdot\delta(Tc)\cdot\ln(Ee) + \beta_{Voc}(Ee)\cdot(Tc-To)\right] \tag{5}$$

$$Vmpg = N_{sg}\left[Vmpo + C_2\cdot N_s\cdot\delta(Tc)\cdot\ln(Ee) + C_3\cdot N_s\cdot\{\delta(Tc)\cdot\ln(Ee)\}^2 + \beta_{Vmp}(Ee)\cdot(Tc-To)\right] \tag{6}$$

$$Pmpg = Impg\cdot Vmpg \tag{7}$$

where Ee is the effective solar irradiance; G is the measured irradiance (W/m^2); G_n is the reference irradiance (1000 W/m^2) at standard conditions (STC); To is the reference cell temperature (25 °C) at STC; Tc is the measured cell temperature inside module (°C); $Isco$ is the PV module short-circuit current at STC (A); α_{Isc} is the normalized temperature coefficient for Isc, (°C^{-1}); $Iscg$ is the PV array short-circuit current (A); N_{pg} is the number of modules connected in parallel; $Impo$ is the PV module current at the maximum power point at STC (A); $Impg$ is the PV array current at the maximum power point (A); α_{Imp} is the normalized temperature coefficient for Imp, (°C^{-1}); C_0 and C_1 are empirically determined coefficients which relate Imp to the effective irradiance, $C_0 + C_1 = 1$, (dimensionless); $\delta(Tc)$ is the thermal voltage per cell at temperature Tc; q is the elementary charge, $1.60218\cdot10^{-19}$ (coulomb); k is the Boltzmann's constant, $1.38066\cdot10^{-23}$ (J/K); n is the diode ideality factor; $Voco$ is the PV module open circuit voltage at STC (V); β_{Voc} is the temperature coefficient for module Voc at standard irradiance, (V/°C); N_s is the number of cells in series per PV module; N_{sg} is the number of modules connected in series; $Vocg$ is the PV array open circuit voltage (V); $Vmpo$ is the PV module voltage at the maximum power point at STC (V); β_{Vmp} is the temperature coefficient for module Vmp at standard irradiance, (V/°C); $Vmpg$ is the PV array voltage at the maximum power point (V); C_2 and C_3 are empirically determined coefficients which relate Vmp to the effective irradiance (C_2 is dimensionless, and the unit of C_3 is (V^{-1}) and finally Pmp is the PV array power at the maximum power point (W).

In order to solve the system equations formed by the Eqs. (1)–(7) and reproduce the behaviour of the whole PV system with a good accuracy, it is necessary to apply specific methods to determine the empirical coefficients. A method based on the combination of indoor and outdoor measurements and coefficients estimation and fitting has been recently reported in the literature (Peng et al., 2015). The set of coefficients used by the model is obtained by means of a parameter extraction procedure carried out in MATLAB/Simulink environment by using the Parameter Estimation toolbox. The monitored current and voltage of the PV array together with in-plane irradiance (G) and cell temperature (Tc) profiles are needed to estimate the set of unknown parameters of SAPM model implemented in Simulink as illustrated in Fig. 1.

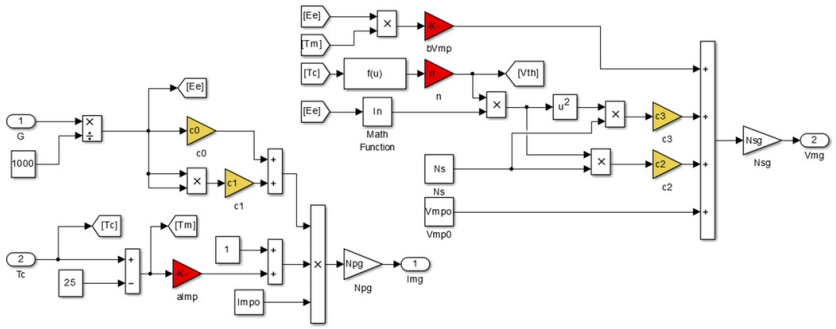

Fig. 1 Simulink block diagram of the parameter extraction algorithm.

The parameter extraction algorithm evaluates: C_0, C_1, C_2, C_3, α_{Imp}, β_{Vmp} and n by using Eqs. (3) and (6). A nonlinear regression method based on the Levenberg–Marquardt algorithm was applied to both data sets: The daily monitored data from the PV array in real conditions of work and the simulation results generated by using the described model of Sandia, in order to minimize the quadratic error between the simulation results and the experimental data.

2.3 Fault detection procedure

The fault detection procedure is based on the analysis of the current and voltage indicators for fault detection, *NRc* and *NRv* respectively, defined by ~~Silvestre et al.~~ Silvestre et al. (2014) and given by the following equations:

$$NRc = \frac{I_m}{I_{scg}} \tag{8}$$

$$NRv = \frac{V_m}{V_{ocg}} \tag{9}$$

where Vm and Im are the coordinates of the maximum power point (MPP) at the DC side of the PV array.

The fault detection algorithm evaluates both *NRc* and *NRv* indicators through MPP coordinates available from the monitoring data set in real time, and the values of I_{scg} and V_{ocg}, obtained for actual conditions of irradiance and temperature by using the PV array model presented in the previous section. Two more parameters can be also obtained from the model simulations in real time: I_{mpo} and V_{mpo}, the current and voltage at the maximum power point of the output of the PV array in absence of faults and normal operation of the PV array (Silvestre et al., 2014). Then, the expected values of *NRc* and *NRv*: *NRco* and *NRvo*, are given by:

$$NRco = \frac{I_{mpo}}{I_{scg}} \tag{10}$$

$$NRvo = \frac{V_{mo}}{V_{ocg}} \tag{11}$$

Silvestre et al. defined two thresholds for current, *TNRcfs*, and voltage indicators, *TNRvbm*, that allow detecting most important faults in grid connected PV systems: short circuits and open circuits in the PV array (Silvestre et al., 2014) as well as inverter disconnection or partial shading conditions of work (Silvestre et al., 2015). These thresholds were defined by the following equations:

$$TNRcfs = 1.02\alpha NRco \tag{12}$$

$$TNRvbm = 1.02\beta NRco \tag{13}$$

where α and β are the relationship between the ratios of current in case of one faulty string and fault-free operation and the ratio between the voltage ratios in case of one bypassed PV module in a string of the PV array and fault-free operation respectively (Silvestre et al., 2014, 2015).

Both parameters depend only on the PV array configuration: Number of PV modules connected in series by string, N_{sg}, and number of strings connected in parallel, N_{pg}. In case of permanent faults in the PV array, short circuits or open circuits, the corresponding current or voltage indicator always remains below its threshold and their effect on the current and voltage ratios is permanent, while in case of partial shading conditions of work or inverter disconnection to prevent islanding, these indicators change as quickly as do the shadows in the photovoltaic field or as soon as the inverter is reconnected to the grid. The islanding refers to the condition in which the PV generator continues to power a location even though power from the electric utility is no longer present. This situation can be dangerous to utility workers. So, the inverter must be disconnected from the grid to avoid islanding when important

frequencies of voltage disturbances are observed.

The fault detection algorithm is able to detect all those faults and generate alarm signals to indicate the most probably fault present in the system. Moreover, the total amount of power losses caused by the fault as well as the equivalent number of short circuited or bypassed PV modules present in the PV array are also evaluated by the fault detection algorithm. The equivalent number of faulty strings, E*fs*, is evaluated by using the following equation (Silvestre et al., 2015):

$$Efs = Npg\left(1 - \frac{NRc}{NRco}\right) \tag{14}$$

Finally, the number of equivalent bypassed modules, *BP*mod, present on the PV array is estimated as follows:

$$BP\text{mod} = Nsg\left(1 - \frac{NRv}{NRvo}\right) \tag{15}$$

The proportion of DC power losses due to the shadowing effect, *Ploss*, is also evaluated by the automatic supervision procedure by using the following equation:

$$Ploss = \left(1 - \frac{NRc}{NRco}\frac{NRv}{NRvo}\right) \tag{16}$$

The efficiency parameters used for the energetic evaluation of the system are the performance ratio (*PR*) and the array yield (Y_a) given by the following equations:

$$Y_a = \frac{\int_0^{\Delta t} P_{ac}\,dt}{P_o} \tag{17}$$

where P_{ac} is the output power of the PV array and P_o is the nominal power of the array.

$$PR = \frac{Ya}{Yr} \tag{18}$$

where *Yr*, is the daily total irradiation H in the array plane divided by the reference daily irradiance at STC.

3 Results and discussion

The operation of a PV plant located in San Sebastián (Gipuzkoa, Spain), which is at latitude of 43° is analysed. Table 1 shows the details of the PV system and main PV module parameters used are given in Table 2.

Table 1 PV system description.

Main parameters	PV system
PV module	IS 160
Nominal power	14.08 kWp
Number of inverters	3
Modules per inverter	28/30/30
Modules in series (*Nsg*)	14/15/15
Strings in parallel (*Npg*)	2/2/2
Tilt	20°
Orientation	9° East
Inverters	Ingecon SUN 5 Single-phase inverter
Inverters nominal power	5 kWp

Table 2 Main parameters of PV modules.

PV module parameters	PV module IS 160
Isc (A)	9.46
Voc (V)	22.2
Current at maximum power point: Impp (A)	8.65
Voltage at maximum power point: Vmpp (V)	18.5
Temperature coefficient of Voc: β_{Voc} (V/°C)	−0.084
Temperature coefficient of Isc: α_{Isc} (A/°C)	$4.60 \cdot 10^{-3}$

This system was remotely supervised and daily evaluated by means of the OPC system. When discrepancies between expected and actual values are observed, the fault detection analysis previously described is applied. This analysis was carried out for the month of December 2014.

The result of the parameters extraction algorithm presented in section 2.2 is the set of empirical coefficients of the SAPM: C_0, C_1, C_2 and C_3, and PV module parameters: α_{Imp}, β_{Vmp} and n, that allow the best approach to the daily evolution of output current and voltage of the PV array. The values of main model parameters obtained by using the parameter extraction algorithm for the PV system under study are given in Table 3.

Table 3 Values obtained for model parameters.

C_0	C_1	C_2 (V^{-1})	C_3	α_{Imp} (1/°C)	β_{Vmp} (V/°C)	n
0.90336	0.002202	3.8319	99.94	$3.768\ 10^{-4}$	−0.10447	1.1003

Figs. 2 and 3 illustrate the daily monitored profiles of irradiance and cell temperature of the PV array used as input data for the parameter extraction algorithm.

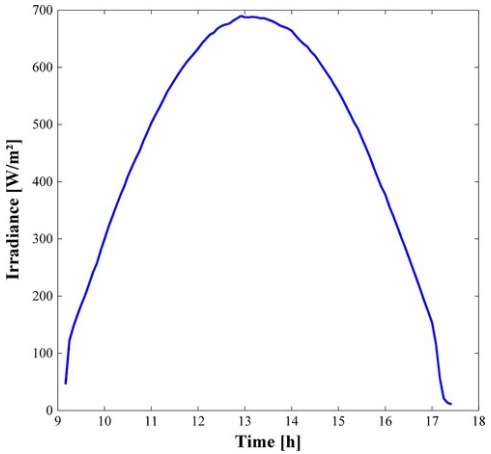

Fig. 2 Irradiance profile corresponding to 10th of December, 2014.

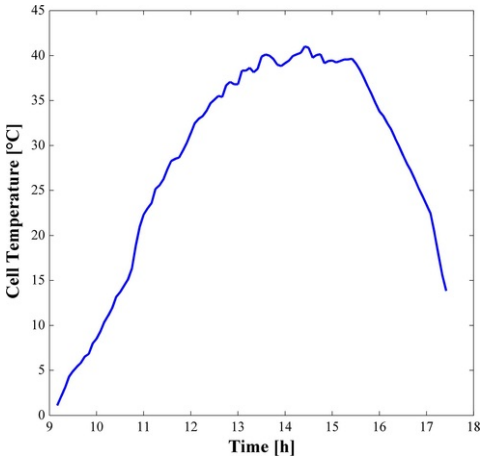

Fig. 3 Cell temperature corresponding to 10th of December, 2014.

Figs. 4 and 5 show the electrical monitored DC output current and voltage, compared with the predicted results obtained by using the set of the model parameters evaluated by the parameter extraction algorithm. The DC output power of the PV array is obtained as a product of current and voltage in both real and simulated results and the obtained result is illustrated in Fig. 6.

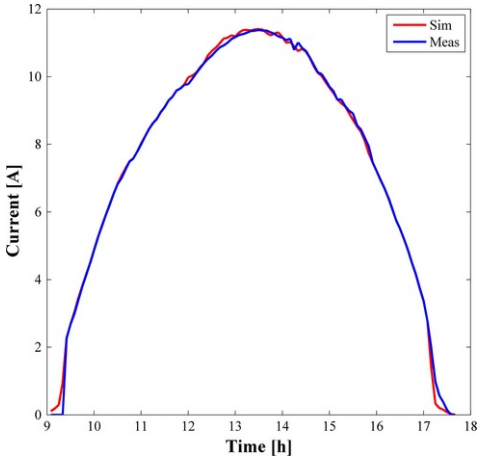

Fig. 4 Simulated and measured DC output Current corresponding to 10th of December, 2014.

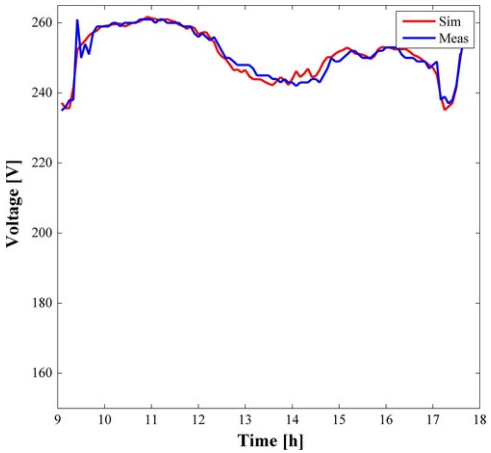

Fig. 5 Simulated and measured DC output voltage corresponding to 10th of December, 2014.

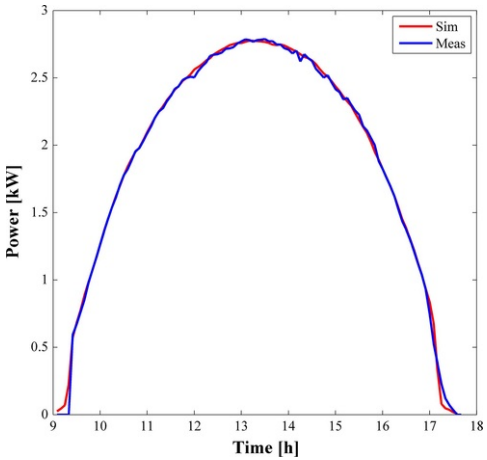

Fig. 6 Simulated and measured DC output Power corresponding to 10th of December, 2014.

As it is shown in Figs. 4–6, a good accordance is obtained between simulation results and the real measured data. The simulation performance was also evaluated by calculating the root mean square errors (RMSEs) of current, voltage and power between both data sets for different days with different climatic conditions.

Table 4 shows the RMSE values obtained. As it can be seen in the table, there is a good agreement between predicted and measured outputs. Furthermore, the inverters connected to the PV array require a minimum input voltage (start-up voltage) to start working. A minimum level of irradiance on the PV array is necessary to enable the proper operation of the inverters. For that reason, a minimum level of G = 200 W/m^2 is considered to start the fault detection evaluation procedure. The RMSE for current, voltage and power were evaluated after filtering the data and run the simulations for irradiance values over the selected threshold of 200 W/m^2.

Table 4 Obtained RMSE (%) for different weather conditions.

Days	RMSE current (%)	RMSE voltage (%)	RMSE power (%)
Clear sky day (G>=200)	0.635	1.229	0.677

Semi cloudy day (G>=200)	0.889	1.284	1.693
Cloudy day (G>=200)	2.573	3.591	3.397

The PV system included in this study was remotely supervised by means of the OPC system. The fault detection procedure described previously is used for analysing the present discrepancies between expected and actual values of the monitored parameters.

From the analysis carried out for the month of December 2014, Fig. 7 shows the evolution of the monitored daily yields and the expected daily yields, Ya-exp, obtained from the modelling of the PV system. As described in Section 2.1, this PV system is formed by three PV arrays connected to three single-phase inverters with a nominal power of 5 kW each one. As shown in Table 1, the subgenerator 1 connected to the inverter 1 has 14 PV modules per string instead of 15. So, the subgenerator 1 has two PV modules least in the PV field that the other inverters.

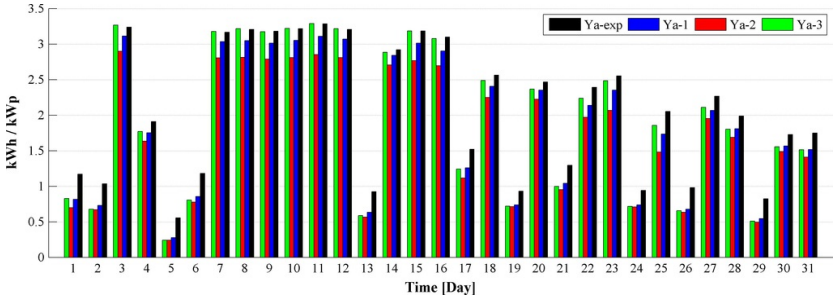

Fig. 7 Daily array yields corresponding to December 2014.

As can be seen in Fig. 7 the daily yields corresponding to the inverter 3, Ya-3, are very similar to the expected daily yields, Ya-exp, evaluated by the model in most of the days, while the yields corresponding to inverters 1 and 2, Ya-1 and Ya-2 respectively, are lower than Ya-3 and Ya-exp. Furthermore the sub-generator connected to the inverter 2 presents the lowest yield in all the days of the month.

In order to analyse possible faults present in the PV system, data corresponding to December 11th was selected to show how the process performs analysis of fault detection. Figs. 2 and 3 show the irradiance and temperature profiles measured on this day of December.

Table 5 shows the daily energy generated by each sub-generator of the PV system (DC and AC) as well as the performance ratio (*PR*).

Table 5 Values of the *PR* and energy generated by the PV system 11th of December, 2014.

	Daily *PR* (%)	Daily DC energy (kW h)	Daily AC energy (kW h)
Sub-generator 1	73.03	13.928	13.026
Sub-generator 2	66.96	13.683	12.797
Sub-generator 3	76.44	16.366	14.609

As it can be seen in Table 5, the sub-generator connected to the third inverter presents the highest value of *PR*, as it might be expected regarding the values of the yields shown in Fig. 7. On the other hand, the *PRs* corresponding to the sub-generators 1 and 2 are lower, especially the *PR* of the second array. This fact, together with low yields values shown in Fig. 7 for sub-generators 1 and 2, indicates some problems present in the PV arrays in this time period. It is necessary to study the evolution of current and voltage indicators to identify the cause of these problems.

As mentioned above, the fault detection algorithm is performed to values of irradiance greater than G = 200 W/m^2, corresponding approximately from 10.00 a.m. to 17.00 p.m. As it can be seen in Fig. 2, the irradiance sensor did not detect any important shadow along the day. However, partial shadows on the sub-generators 1 and 2 were identified by the supervision procedure. The shadow did not cover the sensor irradiance, but a part of the PV generator was affected.

The sub-generator 1 is affected by shadows at the beginning and also at the end of the day. Fig. 8 shows that between 10.00 a.m. and 11.00 a.m. as well as from 16.00 p.m. to 17.00 p.m. the voltage indicator, *NRv*, is below the threshold *TNRbpm* and up to 2.5 PV modules are bypassed as effect of a partial shadow on the array. The number of bypassed PV modules is not an integer because three bypass diodes are included in each of the PV modules present in the PV array. This effect causes a reduction on the output voltage of the PV generator and also a reduction of the output current that is clearly identified by the current indicator analysis shown in Fig. 9. Both indicators *NRc* and *NRv* demonstrate that the sub-generator 1 is highly affected by the shadows in the morning period. At the end of the day, the indicator of current, *NRc*, goes below the threshold, *TNRcfs,* and the reduction in output current is equivalent to one faulty string in this sub-generator.

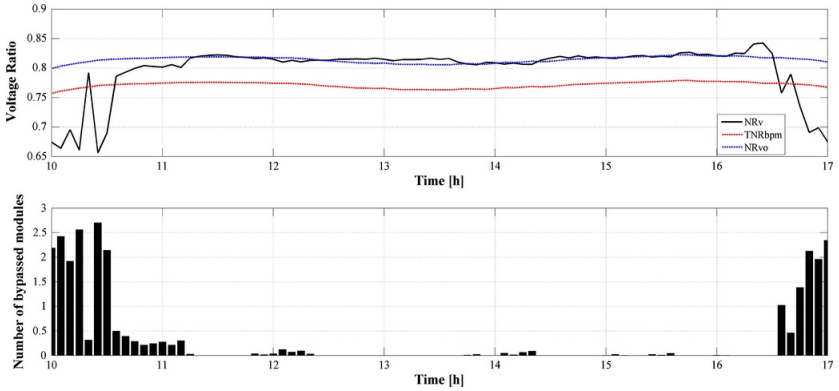

Fig. 8 Sub-generator 1. Evolution of the Voltage ratios and number of bypassed modules.

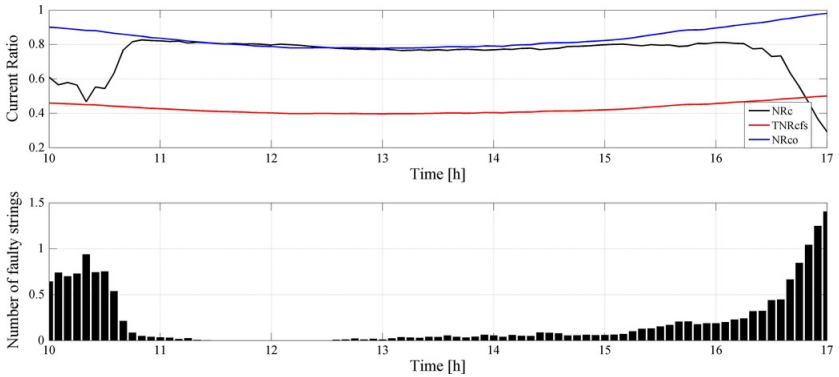

Fig. 9 Sub-generator 1: Evolution of the Current Ratios and equivalent number of faulty strings.

On the other hand, the shadow effects are also the cause of the low *PR* observed in sub-generator 2 indicated in Table 5. In this case the effect is more important. The voltage indicator, *NRv*, appears below threshold, *TNRbpm,* from 10.00 a.m. to 11.00 a.m. and after 15.30 p.m., as it can be seen in Fig. 10. The analysis shows up to seven bypassed modules are detected in the morning and four in the afternoon.

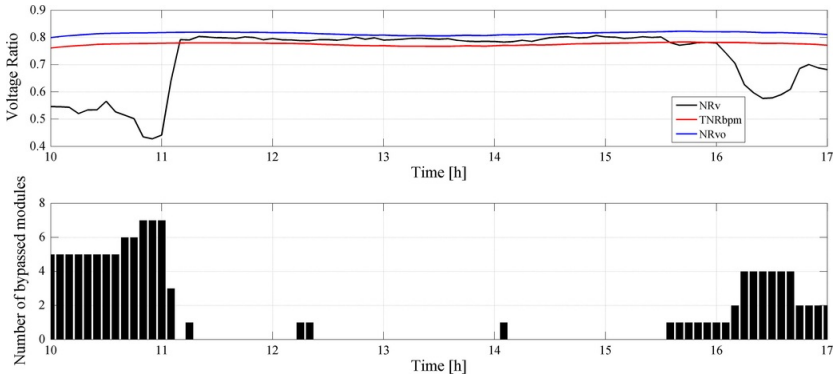

Fig. 10 Sub-generator 2: Voltage ratio and number of bypassed modules.

The evolution of the indicators of current shown in Fig. 11 proclaims a clear reduction in output current in the same periods of time. The effect of shadows on the array of sub-generator 2 is larger than on sub-generator 1 in both cases: Output voltage and current, as it might be expected.

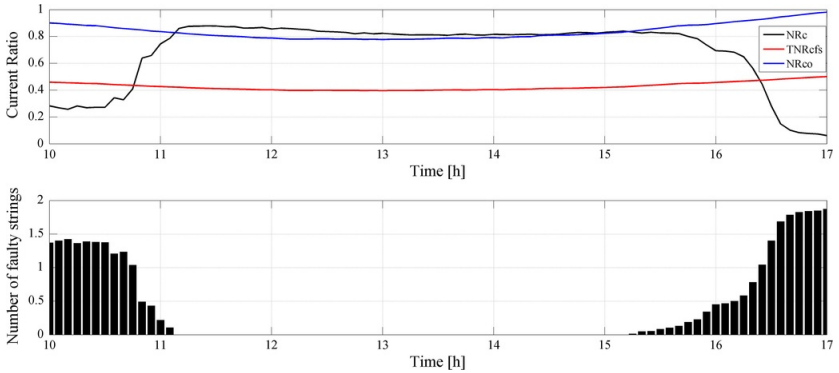

Fig. 11 Sub-generator 2: Current Ratio and equivalent number of faulty strings.

Fig. 12 shows the evolution of voltage indicators. As it can be seen, the sub-generator 3 is working in normal operation without any problem except in the last time of the afternoon, when the voltage indicator, *NRv*, appears below the threshold *TNRbpm* and it seems to be two bypassed modules in the string. The rest of the day there is no reduction in output voltage due to shadows on the array.

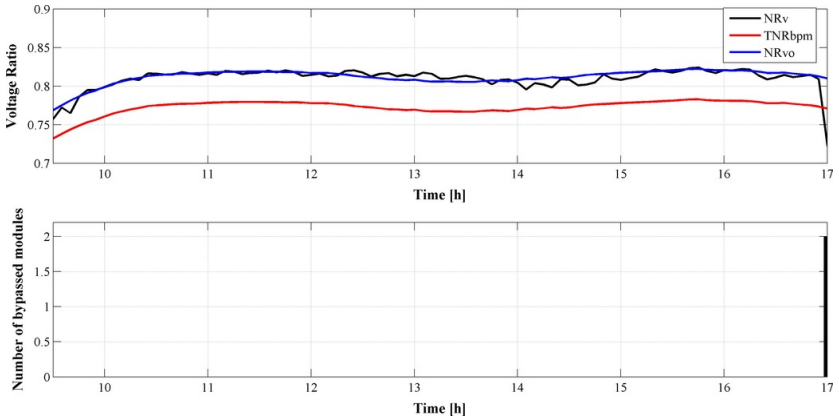

Fig. 12 Sub-generator 3: evolution of the voltage ratios and number of bypassed modules present in the array.

The evolution of the current indicator *NRc* given in Fig. 13 is very similar to the expected value of *NRco* in free fault operation. The current shows a small reduction at the end of the afternoon. However, the indicator of current, *NRc,* remains over the corresponding threshold, *TNRcfs*, and no faulty strings are observed throughout the day.

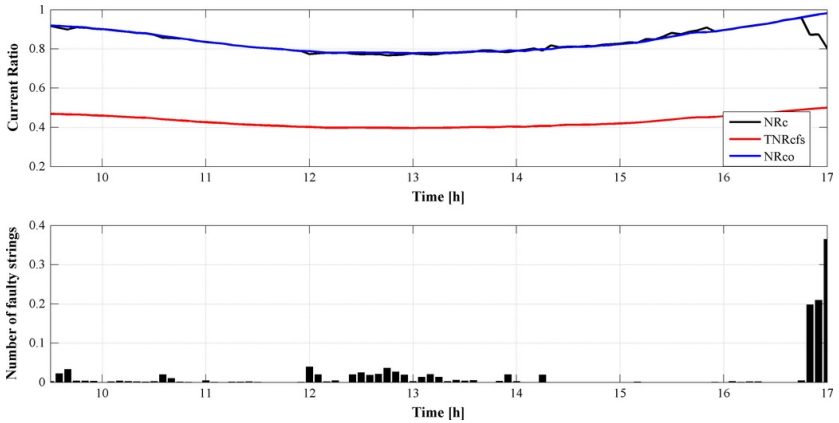

Fig. 13 Sub-generator 3: Current ratio and equivalent number of faulty strings.

The evolution of *Ploss* along the day, evaluated using Eq. (16), is given in Fig. 14 for the three sub-generators. It must be noted that, as it might be expected, the sub-generator that presents the most important reduction in output power is the sub-generator 2, with a total reduction of a 32.76% with respect to the expected output power under normal conditions of operation due to the partial shadows on the array at the beginning and also at the end of the day. Sub- generator 1 shows also reduction in output power in the same periods of time. However, the effect due to shadowing is lower and the total reduction in output power is of a 21.41% with respect to the expected one. Finally, sub-generator 3 is the array showing the lowest power losses.

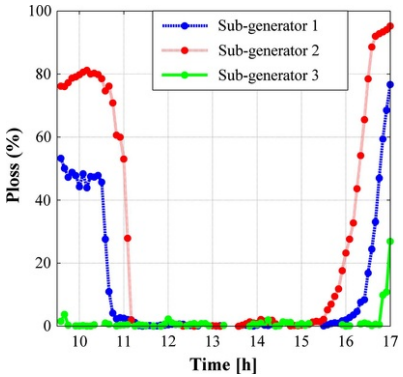

Fig. 14 Estimated power losses.

The results obtained by using the fault detection analysis by means of OPC monitoring for the rest of the month are very similar to the ones presented as example for December 11th. Neither disconnections of inverters to prevent islanding nor permanent faults in the PV system were detected during the period analysed. The shading effects observed in sub-generator 2, in the morning and afternoon, appear throughout all the month and are responsible for most losses of the PV generation system. Sub-generator 1 is also affected by partial shading at the beginning and at the end of the day, but in this case the duration is shorter and the effect in the total reduction of output power is minor. The repetition of the pattern of shadows in the sub-generators 1 and 2 indicates that the effect of nearby obstacles or even the effect of the shadow of a string of PV modules on another string is its most likely origin. Finally, sub-generator 3 presents the best behaviour and daily yields, being the least affected by shadows.

4 Conclusions

In this work a procedure for remote supervision and diagnosis of grid connected PV systems by means of OPC monitoring is presented. Monitoring, supervision and fault detection of the PV system are integrated in the same environment.

The supervision is based in the comparison of the monitored data with the expected evolution of the output current, voltage and power of the PV system. In order to obtain the data set corresponding to the expected behaviour of the PV system for actual irradiance and temperature profiles a model of the PV generator is needed. An empirical model is used for this purpose in combination with parameter extraction techniques. The experimental validation results indicated that the model can accurately evaluate the values of output current, voltage and power of the PV system in real conditions of work practically in real time. The RMSE between real monitored data and results obtained from the modelling of the PV array were below 3.6% for all parameters even in cloudy days.

The fault detection procedure used for the diagnosis of the PV system is based on the analysis of the current and voltage indicators evaluated also from monitored data and expected values of current and voltage obtained from the model of the PV generator. Finally the remote supervision and diagnosis procedure were experimentally verified in real conditions of work in a grid connected PV system formed by three sub-generators connected to inverters with a nominal power of 5 kW each. Results obtained show that the proposed methodology is effective and offers a powerful tool in the field of remote supervision and control of PV systems connected to the grid.

References

Alan Gordon. Programación COM y COM+. Anaya Multimedia, 2001.

Chine W., Mellit A., Pavan A.M. and Kalogirou S.A., Fault detection method for grid connected photovoltaic plants, *Renew. Energy* **66**, 2014, 99–110.

Chouder A. and Silvestre S., Automatic supervision and fault detection of PV systems based on power losses analysis, *Energy Convers. Manage.* **51**, 2010, 1929–1937.

Coleman A. and Zalewski J., Intelligent fault detection and diagnostics in solar plants, In: *Intelligent Data Acquisition and Advanced Computing Systems (IDAACSs),* 2011, 948–953.

Drews A., De Keizer A.C., Beyer H.G., Lorenz E., Betcke J., Van Sark W.G.J.H.M., Heydenreich W., Wiemken E., Stettler S., Toggweiler P., Bofinger S., Schneider M., Heilscher G. and Heinemann D., Monitoring and remote failure detection of grid connected PV systems based on satellite observations, *J. Sol. Energy* **81**, 2007, 548–564.

Firth S.K., Lomas K.J. and Rees S.J., A simple model of PV system performance and its use in fault detection, *Sol. Energy* **84**, 2010, 624–635.

Holley D.W., Understanding and using OPC maintenance and reliabi- lity applications, *Comput. Contr. Eng. J.* **15** (1), 2004, 28–31.

Jarque C.M., Bera A. and Anil K., A test for normality of observations and regression residuals, *Int. Stat. Rev.* **55** (2), 1987, 163–172.

King D.L., Kratochvil J.A. and Boyson W.E., Photovoltaic Array Performance Model, 2004, Department of Energy; USA.

Leloux J., Narvarte L., Luna A. and Desportes A., Automatic fault detection on BIPV systems without solar irradiation data, In: *Proc. of the: 29th European Photovoltaic Solar Energy Conference and Exhibition,* 2014, 1–7.

Liu J., Lim K.W., Ho W.K., Tan K.C., Tay A. and Srinivasan R., Using the OPC standard for real-time process monitoring and control, *IEEE Softw.* **22** (6), 2005, 54–59.

Martínez-Marchena I., Marco de trabajo para la generación de software para la gestión de sistemas de energía solar, Universidad de Málaga, PhD Thesis2015, Universidad de Málaga, junio.

Martinez-Marchena I., Mora-Lopez L., Sanchez P.J. and Sidrach-de-Cardona M., Binding machine learning models and OPC technology for evaluating solar energy systems, *Lect. Notes Comput. Sci.* **6098**, 2010, 606–615.

Martínez-Marchena Ildefonso, Sidrach-de-Cardona Mariano and Mora-López Llanos, Framework for monitoring and assessing small and medium solar energy plants, *J. Sol. Energy Eng.-Trans. ASME* **137** (2), 2014, 021007.

Peng J., Lu L., Yang H. and Ma T., Validation of the Sandia model with indoor and outdoor measurements for semi-transparent amorphous silicon PV modules, *Renew. Energy* **80**, 2015, 316–323.

Silvestre S., Aires da Silva M., Chouder A., Guasch D. and Karatepe E., New procedure for fault detection in grid connected PV systems based on the evaluation of current and voltage indicators, *Energy Convers. Manage.* **86**, 2014, 241–249.

Silvestre S., Kichou S., Chouder A., Nofuentes G. and Karatepe E., Analysis of current and voltage indicators in grid connected PV(photovoltaic) systems working in faulty and partial shading conditions, *Energy* **86**, 2015, 42–50.

Vergura S., Acciani G., Amoruso V., Patrono G.E. and Vacca F., Descriptive and inferential statistics for supervising and monitoring the operation of PV plants, *IEEE Trans. Ind. Electron.* **56–11**, 2009, 4456–4464.

Wu Y., Lan Q. and Sun Y., Application of BP neural network fault diagnosis in solar photovoltaic system, In: *Mechatronics and Automation (ICMA),* 2009, 2581–2585.

Highlights

- Standard OPC for monitoring and supervision of grid connected PV systems is applied.
- An empirical model ~~in combination with parameter extraction techniques~~ is used to obtain the ~~expected~~ evolution of main PV system parameters.
- The RMSE ~~errors between real monitored data and results~~ obtained ~~from the modelling of the PV array~~ were less than 3.6% for all parameters even in cloudy days.
- A powerful tool for remote supervision and control of PV ~~generation~~ systems ~~connected to the grid~~ is presented.

Queries and Answers

Query: Your article is registered as a regular item and is being processed for inclusion in a regular issue of the journal. If this is NOT correct and your article belongs to a Special Issue/Collection please contact j.aranha@elsevier.com immediately prior to returning your corrections.
Answer: It is correct

Query: The author names have been tagged as given names and surnames (surnames are highlighted in teal color). Please confirm if they have been identified correctly.

Answer: The surnames are correct

Query: Highlights should only consist of 85 characters per bullet point, including spaces. The highlights provided are too long; please edit them to meet the requirement.
Answer: The highlights have been modified.

Query: Please note that the reference style has been changed from a Numbered style to a Name–date style as per the journal specifications.
Answer: OK